

3D printed polycaprolactone-microcrystalline cellulose scaffolds

M.E. Alemán-Domínguez,¹ E. Giusto,² Z. Ortega,¹ M. Tamaddon,² A.N. Benítez,¹ C. Liu²

¹Departamento de Ingeniería de Procesos, Universidad de Las Palmas de Gran Canaria, Edificio de Fabricación Integrada, Parque científico-tecnológico de la ULPGC, Las Palmas (Spain)

²Institute of Orthopaedic & Musculoskeletal Science, University College London, Royal National Orthopaedic Hospital, Stanmore HA4 4LP, London (United Kingdom)

Abstract

Microcrystalline cellulose (MCC) is proposed in this study as an additive in polycaprolactone (PCL) matrices to obtain 3D printed scaffolds with improved mechanical and biological properties. Improving the mechanical behavior and the biological performance of polycaprolactone-based scaffolds allows to increase the potential of these structures for bone tissue engineering.

Different groups of samples were evaluated in order to analyse the effect of the additive in the properties of the PCL matrix. The concentrations of MCC in the groups of samples were 0, 2, 5 and 10% (w/w). These combinations were subjected to a thermogravimetric analysis in order to evaluate the influence of the additive in the thermal properties of the composites.

3D printed scaffolds were manufactured with a commercial 3D printer based on fused deposition modelling. The operation conditions have been established in order to obtain scaffolds with a 0/90° pattern with pore sizes between 450-500 µm and porosity values between 50-60%. The mechanical properties of these structures were measured in the compression and flexural modes. The scaffolds containing 2% and 5% MCC have higher flexural and compression elastic modulus, although those containing 10% do not show this reinforcement effect. On the other hand, the proliferation of sheep bone marrow cells on the proposed scaffolds was evaluated over 8 days. The results show that the proliferation

is significantly better ($p < 0.05$) on the group of samples containing 2% MCC. Therefore, these scaffolds (PCL:MCC 98:2) have suitable properties to be further evaluated for bone tissue engineering applications.

Keywords: Biocompatibility/hard tissue, bone marrow, porous, tissue engineering, bone remodeling

Running head: 3D printed polycaprolactone-microcrystalline cellulose scaffolds

Introduction

Population ageing is a major demographic concern, as it is expected that in 2050 the number of citizens over 60 years old is about 2 billion ¹. For this reason, there is an increasing interest in the development of innovative strategies to treat bone injuries and diseases that come with the ageing population. One of the most promising ones is bone tissue engineering.

Tissue engineering is a multidisciplinary field involving medicine, materials engineering, mechanical engineering, biology, among others. Its main goal is developing biological substitutes to replace, regenerate or improve the functionality of injured or damaged tissue. To create such a substitute (scaffolds), it is necessary to have a support material able to promote and enhance the attachment and proliferation of the cells that will carry out the biological functions. The techniques based on additive manufacturing have been widely explored because they offer the possibility of creating 3D scaffolds with controlled porosity and a customized design.

One of the most common materials in the manufacturing of scaffolds for bone regeneration by additive manufacturing is polycaprolactone ². Polycaprolactone (PCL) is a linear polyester with good biocompatibility, a relatively slow degradation rate and ease of processability ³. These characteristics are suitable for the usage of this polymeric material in tissue engineering applications ⁴⁻⁷. However, surface cell attachment on the structures is limited because of the hydrophobic nature of the material ^{3,8,9}. In addition to the low bioactivity of PCL, this thermoplastic material has worse mechanical properties than other biopolymers suitable for tissue engineering. For instance, the flexural modulus of PCL is 0.48-0.58

GPa compared to the modulus of polylactic acid (PLA) (3.1-3.6 GPa),¹⁰ another material commonly used in this type of applications, showing that PCL does not mimic the mechanical properties of the surrounding tissue as well as PLA.

Several authors have proposed the formulation of composites based on a PCL matrix to overcome this limitation. For instance, Ródenas et al.¹¹ have evaluated how hydroxyapatite can enhance cell adhesion and simultaneously acts as a reinforcement. Other substances proposed to create a hybrid material through their combination with polycaprolactone are graphene oxide¹², calcium carbonate^{13,14} or gelatin¹⁵.

In this study, microcrystalline cellulose has been proposed as an innovative additive to be used as filler in a polycaprolactone matrix to obtain a composite material able to be processed by additive manufacturing techniques in order to improve the mechanical behaviour and the biological response compared to pure polycaprolactone. Several studies have reported the utilization of cellulose as support material in tissue engineering. For example, Jia et al.¹⁶ have proposed the utilization of microcrystalline cellulose and cellulose whiskers to obtain electrospun scaffolds able to support the growth of vascular smooth muscle cells.

However, no references have been found proposing the combination of this substance with polycaprolactone to create a composite material that can be processed by 3D printing techniques. In this study, this strategy has been explored by manufacturing scaffolds by 3D printing based on fused deposition modelling.

Materials and methods

Materials

Polycaprolactone (PCL) Capa ® 6800 with mean molecular weight 80,000 Da, melting point of 58-60°C and melt flow index of 4.03-2.01 g/10 min was kindly supplied by Perstorp, UK. Microcrystalline cellulose (MCC) was purchased from Sigma Aldrich. The following reagents were used for cell culture:

DMEM low glucose (Sigma-Aldrich, UK), 100 units/ml penicillin-streptomycin (P/S, Gibco, UK), PBS (Life Technologies), fetal calf serum-columbia (First Direct, First Link, UK), trypsin-EDTA (0,5%) (Thermo Fisher Scientific).

Preparation of composite materials and scaffolds manufacturing

PCL pellets were milled at 8000 rpm in an Ultra Centrifugal Mill ZM 200 Retsch. This powder was mixed with the amount of powder of MCC needed to obtain PCL:MCC 98:2, 95:5, 90:10 and 80:20 (wt:wt) mixtures. After homogenization, the mixture was subjected to compression moulding in a Collin P 200 P/M press. The cycle used consisted of a first step of heating at 20°C/min up to 85°C at constant pressure of 10 bar, keeping the temperature and the pressure for 2 min and subsequent cooling until room temperature at 20°C/min.

PCL, PCL:MCC 98:2, PCL:MCC 95:5 and PCL:MCC 90:10 sheets were obtained by compression moulding. These sheets were then cut into small rectangle shaped pieces to use them as pellets, fed into an extruder to obtain a continuous filament needed to print parts by fused deposition modelling. This extruder consists of an 8 mm screw and cylinder with a L/D ratio of 10 and a nozzle tip of 1.6 mm. The extrusion was carried out at 120°C and at a rotating speed of 7 rpm. This temperature was changed for blends containing 10% of microcrystalline cellulose. It was increased up to 130°C to obtain a more suitable flow of the material through the nozzle.

The filaments obtained were used to print the parts needed for the different tests described in this report with a Prusa i3 3D printer. The temperature used to print the structures was 210°C. Structures with a rectangular 0/90° pattern were printed to carry out the mechanical, morphological and biological characterization of the composite scaffolds. This pattern provides square shaped pores in an interconnected network that ensures a suitable vascularization of the structure.

Thermogravimetric analysis

The pellets of pure PCL and composite PCL:MCC materials (98:2, 95:5 and 90:10) were subjected to thermogravimetric scans in a TGA/DSC 1 Mettler Toledo device. A cycle of heating up to 600°C at a heating rate of 20°C/min with an air flow of 10 ml/min was followed in each case, using aluminium crucibles. The experiments were carried out in triplicate to obtain the degradation profile of the composites. The same procedure was followed to analyse pure MCC powder. During the TGA testing it is possible to obtain the calorimetric data using the same thermal cycle. This data allowed determining the melting temperature of the hybrid materials and their melting enthalpy.

The values of the melting enthalpy were used to calculate the crystallinity of the samples by applying the following equation:

$$X_c = \left(\frac{\Delta H_m}{\Delta H_m^0 \cdot (1 - x_{MCC})} \right) \cdot 100$$

Where ΔH_m^0 is the enthalpy of fusion of PCL 100%. The value of this parameter used in this study was 142.0 J/g ¹⁷.

Infrared characterization

Fourier-transformed infrared (FTIR) spectra were obtained in the attenuated total reflectance (ATR) mode using a Perkin Elmer IR Spectrum Two with wavelengths from 4000 to 450 cm⁻¹ at 8 cm⁻¹ resolution. 12 scans per measurement were used to obtain the average spectra. For each sample, five measurements were carried out.

The area of the of the peak of the CH₂ group at 2945 cm⁻¹ and the area of the C-O-C group at 1245 cm⁻¹ were measured with the Spectrum10 software.

According to Phillipson ¹⁸, the asymmetric stretching peak of the CH₂ group at 2945 cm⁻¹ in the PCL structure has a medium intensity in the amorphous phase (very weak in the crystalline one) and the symmetric stretching peak of the C-O-C group at 1245 cm⁻¹ has a medium intensity in the crystalline

phase, but weak when it is in the amorphous phase. Hence, the ratio between the areas of these two signals can be used as an indicator of the relative abundance of both crystalline phases.

Morphology

The surface of the scaffolds was observed with a desktop scanning electron microscope (SEM) Hitachi TM 3030 at an acceleration voltage of 15 kV. The samples were sputtered with Pd/Au for 2 minutes at 18 mA in a Polaron SC7620 sputter.

On the other hand, the porosity of the structures was evaluated according to the following equation. This method has been broadly used in the literature to evaluate the porosity of 3D printed scaffolds^{2,19}.

$$\%porosity = 100 \cdot \left(1 - \frac{\rho_{ap}}{\rho_{bulk}}\right)$$

Where ρ_{ap} is the apparent density of the structure and ρ_{bulk} is the density of the bulk material. The density of the bulk material was determined by measuring the dimensions of short filaments of material with a cantilever ($\pm 0,01$ mm) and their mass (n=8). On the other hand, the apparent density was measured following a similar protocol with 3D printed scaffolds of $13 \times 13 \times 8$ mm³ of nominal dimensions.

As the printing pattern was 0/90°, the pore size was evaluated as the distance between filaments. These values were measured with the software of an optical microscope Olympus BX51 (n=36).

Mechanical properties

The mechanical characterisation of the 3D printed structures was carried out in order to evaluate the effect of the introduction of microcrystalline cellulose. The flexural and compression modulus and the stress at yield point were measured. For the flexural properties, the 3 point bending testing was carried out. Five replicas of 3D printed samples were used to obtain the flexural parameters of the structures made with different blends of material. The area tested were rectangles of $17 \times 9 \times 2.6$ mm. This

characterization was carried out using a Zwick Roell Z005 machine in displacement control mode at a crosshead speed of 1 mm/min. The parameters were calculated according to the procedures explained in the standard ASTM D790-15.

Regarding the compression properties, four replicas of printed samples of 4x4x8 mm were subject to compression in a Zwick Roell Z0.5 device at a crosshead speed of 1 mm/min. The compressive modulus was calculated from the initial steepest straight line portion of the load-strain curve according ASTM D1621-16. On the other hand, the load at the yield point was evaluated as the first point on the stress-strain diagram where an increase in strain occurs without an increase in stress.

In vitro cell seeding

Bone marrow mesenchymal stem cells were harvested from sheeps. In brief, 5 ml of bone marrow was collected in a tube with 250 ul of heparin. The bone marrow aspirate was transferred to a T225 cell culture flask (Corning, Thermo Fisher Scientific UK) together with DMEM low glucose supplemented with 1% penicillin-streptomycin (10000 U/ml) and 10% fetal calf serum. After 3 days, the cells were washed with phosphate buffered saline and new culture media was added to the flask. Once the flask reached 80-90% confluency, the cells were detached with trypsin-EDTA (0,5%), counted and re-plated with culture medium that was renewed every two days.

8 mm diameter cylindrical scaffolds were cut using 8mm biopsy punch (Kai Medical) to be used as substrate for the cell culture. Two replicas of each type of scaffold (PCL, PCL:MCC 98:2, PCL:95:5, PCL:MCC 90:10) were seeded with a dynamic process. 1 ml suspension of 150,000 cells was introduced in a sterile tube with each sample. The tubes were placed in a tube rotator (MACSmix, Miltenyi Biotec) rotating at 12 rpm on continuous cycle for 1 hour inside an incubator at 37°C and 5% CO₂. This procedure allows the cells to attach to the inside of the scaffold, instead of only on the outer surface. Afterwards, the samples were transferred to a non-treated well plate (Corning, Life Technologies UK) and cultured in the supplemented media described above. This media was refreshed every two days.

Viability tests

The viability of the cells after 1, 3 and 8 days of culturing was evaluated through the resazurin-based Presto Blue® assay (Invitrogen, Thermo Scientific UK) in duplicate for each sample. The samples were incubated in a 10% Presto Blue solution in media for 30 minutes. The negative controls of the assay were composite scaffolds without cells in order to take into account a possible adsorption of the reagent by the microcrystalline cellulose. After the incubation, 100µl of supernatant was transferred to a black 96 well plate in duplicates and the fluorescence of the wells was analysed with a Tecan Infinite 200 Pro microplate reader at the excitation and emission wavelengths of 540 and 590 nm, respectively. The fluorescence values are calculated according to:

$$\text{Mean fluorescence of each group of samples} = \text{Mean (AF-mean NCF)}$$

Where AF is the fluorescence value read for each replica of the group and NCF is the negative control fluorescence.

Statistical analysis

For every quantitative characterization method, the Wilcoxon test was used to evaluate if the data from every group of samples showed a significant difference compared to pure PCL results ($p < 0,05$ for significant and $p < 0,01$ for highly significant statistical difference). The implementation of the Wilcoxon test was carried out with Matlab 7.4. (2007) software (MathWorks). All the figures show the mean values of each group and their standard deviation are represented with error bars.

Results

Thermogravimetric analysis

The thermogravimetric analysis allows to obtain the degradation temperature of the composite materials and to compare these values to pure PCL. This information is useful to establish the maximum value of the operation temperature to be used when processing these materials by any thermal technique,

such as fused deposition modelling. Besides, the calorimetric parameters can be used to evaluate whether the introduction of the MCC implies any changes in the crystallinity of the matrix. The temperature of maximum degradation rate decreases when the microcrystalline cellulose is loaded in the polycaprolactone matrix (from 430°C to 424°C) (Table 1). The PCL melting temperature and enthalpy of fusion increase when a small fraction of MCC is introduced (2 and 5% w/w), but decrease as such fraction grows (10% w/w): the melting temperature is 63°C for pure PCL and it varies between 68 and 70°C for the composites. A similar trend is observed for the degree of crystallinity of the matrix (Table 1): this value increases from the 23% for pure PCL samples up to 31% when the MCC loading is 5% w/w, but it is slightly reduced to 30% when the concentration of the additive reaches 10% w/w.

Infrared characterization

The FTIR spectra have been used to evaluate whether there is a strong interaction between the two components in the composite material (PCL and MCC) or not. Besides, the analysis of the spectra was useful to confirm the changes in the degree of crystallization as complementary information to the calorimetric data (Table 1). Using the FTIR spectra to study the crystallization process of polycaprolactone-based materials is a strategy that has been explored previously in the literature^{20,21}.

The FTIR spectra of the microcrystalline cellulose shows the characteristic peaks of this compound, such as the hydroxyl signal between 3300-3600 cm⁻¹ and the peak of the C-O bond at 1030 cm⁻¹. For all the composites and pure polycaprolactone it is possible to observe the band at 1720 cm⁻¹ attributed to the carbonyl stretching of the ester group^{22,23} and the signal at 2946 and 2870 cm⁻¹ related to the asymmetric and symmetric CH₂ stretching²⁴. (Figure 1)

As it is possible to observe in Figure 1, the carbonyl peak has not been displaced to lower values of the wavenumber, as it is expected on carbonyl groups subjected to additional hydrogen bonding²⁵. This type of bonding could be expected from the interaction between the carbonyl groups in the PCL structure and the hydroxyl groups in microcrystalline cellulose. However, this lack of modification on the

position of the carbonyl peak is an evidence of the absence of relevant intermolecular interactions between the two components in the composites.

On the other hand, the ratio of the areas of the CH₂ and the C-O-C peaks was found to decrease with the microcrystalline cellulose loading. The value of 1.34 for PCL decreases in a highly significant way ($p < 0.01$) to 1.08 for the PCL:MCC 98:2 samples. When the concentration of the additive is 5% w/w, the ratio is 1.19 ($p < 0.05$) and when the concentration is increased up to 10% w/w, the value decreases to a value of 1.14 (Table 2). As previously described, the modification of this ratio is related to the relative amount of the crystalline and the amorphous phase. Hence, the FTIR spectra analysis confirms the increment of the crystallinity of the polycaprolactone matrix with the microcrystalline cellulose loading and it shows that this modification is dependent on the concentration of additive in the composite material.

Morphological evaluations

The presence of microcrystalline cellulose modifies the topography of the 3D printed structures, so the PCL samples have a smoother surface than the composite ones (Figure 2). This effect is strongly dependent on the concentration of microcrystalline cellulose on the samples. As it is possible to observe in Figure 2-b, PCL:MCC 98:2 samples have a topography quite similar to pure PCL scaffolds. On the other hand, the samples containing 5% of MCC have a rough surface, but the morphology of the filaments is steady (Figure 2-c). Finally, when the concentration is increased up to 10% w/w, the deposition process is hindered and the modification of the morphology of the structures affects not only the surface of the filaments, but also their integrity (Figure 2-d).

According to the datasheet of the product, the bulk density of microcrystalline cellulose is 0.6 g/cm³. Hence, if the additive did not affect the properties of the polycaprolactone matrix, the bulk density of the composites should be lower, according to the rule of mixture. However, the bulk density of the material increases with the loading of microcrystalline cellulose for the samples containing 2% and 5% w/w MCC (from the 1.09 g/cm³ up to 1.23 g/cm³, Table 3). When the concentration is increased up to

10%, the value is higher than the pure polycaprolactone, but lower than the values for the groups of samples with a lower concentration (1.13 g/cm³) (Table 3). The apparent density of the scaffolds remains unchanged for all the groups of samples with values between 0.48 and 0.53 g/cm³. On the other hand, the porosity values (between 52-58%, Table 3) are slightly higher in the composite scaffolds, with an increment lower than 10%. The average pore size is between 450-500 μm for all the groups of samples evaluated (Table 3). There is a statistically significant but very slight increment (4% compared to pure PCL) of the distance between filaments (identified herein as pore size) for the samples with 5% w/w content in microcrystalline cellulose.

Mechanical properties

The introduction of MCC increases the flexural modulus by 19% when the concentration added is 2% w/w (from 61 MPa for PCL samples to 72 MPa for PCL:MCC 98:2) and by 25% if the MCC content is raised up to 5% w/w (the modulus reaches 76 MPa in this group of samples). However, the samples with a 10% of additive do not show a significant modification ($p>0,05$) on this mechanical parameter (Figure 3) (with a mean value of 55 MPa). On the other hand, the value of the yield strength remains unchanged between the groups PCL, PCL:MCC 98:2 and PCL:MCC 95:5 (7.2 MPa; 7.1 MPa and 6.9 MPa respectively) but decreases significantly ($p<0.05$) for the PCL:MCC 90:10 group (4 MPa). The value of this parameter is indeed 45% lower than for pure PCL samples (Figure 3).

Regarding the compression properties, the values of the modulus are 25 MPa for pure PCL, 32 MPa for PCL:MCC 98:2, 29 MPa for PCL:MCC 95:5 and 7 MPa for PCL:MCC 90:10 (Figure 4). These values are in the range reported elsewhere for 3D printed polycaprolactone scaffolds^{19,26} and in the interval of values reported for spongy bone (20-500 MPa)²⁷. As described previously for the flexural properties, the value of the compressive modulus increases when the concentration of MCC is 2% and 5% w/w, but decreases when it is 10% w/w (Figure 4). Something similar happens to the stress at yield point. This parameter is 28% higher with a 2% of additive compared to pure PCL samples (2.1 MPa for

pure PCL and 2.7 MPa for PCL:MCC 98:2), but decreases a 4% when the amount of MCC is 10% wt/wt of the blend (1.3MPa).

Biological evaluation of scaffolds

The fluorescence values of the Presto Blue assay for day 1 can be considered as an indirect indication of the cell attachment, as they are related to the amount of cells that have been able to colonize the surface of the samples at the beginning of the cell culture. Therefore, as there is not any significant difference in this value between the groups analyzed (Figure 5), it is possible to confirm that the cellulose loading does not affect cell attachment. However, the proliferation of the cells was found to be increased with the additive when its concentration is kept low (2%). A higher amount of microcrystalline cellulose hinder the proliferation of the cells: the fluorescence values for the PCL:MCC 90:10 samples are significantly lower than those from pure PCL ones (Figure 5).

Discussion

The presence of microcrystalline cellulose was found to slightly decrease the maximum degradation temperature from 429°C (for PCL) to 424°C (for all the composites evaluated). This trend of decrease of the maximum degradation temperature when an additive is loaded in a polycaprolactone matrix has been previously reported for the incorporation of cellulose-based fillers, like agricultural waste²⁸, sisal fiber²⁹ or carboxymethyl cellulose³⁰. Despite the reduction on the degradation temperature, as the melting temperature of all the composites is between 63-70°C (Table 1), there is a wide safe temperature window to process the materials by thermal techniques, such as 3D printing based on fused deposition modeling.

On the other hand, the increase of the crystallinity degree has been confirmed by the calorimetric data (Table 1), by the FTIR analysis (Table 2) and the values of the bulk density of the composite materials (Table 3). This trend can be explained by the nucleation effect caused by the presence of the

microcrystalline cellulose particles. Besides, it is possible to suggest that this increase of the crystallinity explains the reinforcement effect of the additive with low concentrations (2 and 5% w/w).

When the concentration of the filler is increased (up to values of 10% w/w) the particles tend to agglomerate because of the lack of interaction with the matrix. If the particles are agglomerated, the interfacial area available for the particles to act as nucleation points of the thermoplastic is relatively lower. Consequently, the increment of the crystallinity of the matrix is hindered, as it is proved by the crystallinity values obtained in the calorimetric analysis (Table 1).

The FTIR spectra do not show any displacement or modification of the peaks that could confirm some kind of intermolecular interaction between the two components. This lack of interaction is responsible for the agglomeration of the particles of microcrystalline cellulose that explains the decrease on the nucleation effect described herein.

Regarding the structures obtained with the PCL:MCC composites, the apparent density of all the groups of scaffolds is between 0.48 and 0.53 g/cm³ (Table 3). These values are within the range reported for spongy bone: 0.14-1.2 g/cm³ ²⁷. On the other hand, the values of porosity (between 52-58%) are similar to the ones reported for other scaffolds in previous literature for bone regeneration ^{19,31}. The slight increase of the porosity observed in the composite samples (Table 3) could be attributed to the surface microporosity of the filaments (Figure 2). This modification does not affect the mesostructure of the scaffold, so the vascularization is not compromised. However, topographical effects might have an influence on the biological response of the cells during their attachment and proliferation processes.

Regarding the pore size, previous literature has reported that pores between 150-500 μm are suitable for scaffolds to be used in bone regeneration ^{32,33}. The structures obtained in this study fulfill this requirement, as the pore size is between 450-500 μm for all the materials evaluated.

Regarding the mechanical properties of the composite scaffolds, the disappearance of the reinforcement effect when the concentration of the additive is above a limit value is a trend that has been

observed previously on the reinforcement of polycaprolactone with hydroxyapatite and halloysite. The maximum amount of these fillers are 20% for hydroxyapatite ^{10,34} and 7.5% for halloysite ¹⁰. These authors point out that above the limit concentrations, the particles of the filler tend to agglomerate. The agglomerates weaken the composite materials, as they act as initiation points of failure. However, in this case the agglomerations have an additional drawback: they hinder the 3D printing processing (Figure 2). The loss of integrity of the filaments when the concentration of microcrystalline cellulose is 10% w/w hinders the layer-layer adhesion, so the structure is weakened, as confirmed by the data from the mechanical characterisation of the scaffolds.

The cell viability test demonstrates that all the composites evaluated are biocompatible, in terms of cell viability, as the population of cells grows for all the groups (Figure 5). Besides, the introduction of a low concentration of microcrystalline cellulose improves the cell proliferation on the composite scaffolds. A higher amount of additive hinders the proliferation of the cells. Regarding the change of the morphology of the filaments (Figure 2), it is possible to state that the microtopography of these samples may influence the mechanism of cell spreading. Naganuma ³⁵ analyzed how the microtopography can affect the behavior of adherent cells on polylactic acid surfaces. She found that the shape of the micro patterns could direct the attachment of the filopodia and therefore, influence cell orientation and proliferation. However, there is not yet agreement on the mechanism on how the topography has such an influence on cell behavior³⁵⁻³⁷. In this study, the microtopography has a random pattern and, therefore, it is not possible to confirm whether it hinders the cell proliferation, as suggested by the viability test.

Nevertheless, it is possible to confirm that the benefits of the loading is concentration-dependent both in terms of mechanical properties and bioaffinity. A similar trend has been reported previously for polylactic acid filled with Bioglass® ³⁸ or hydroxyapatite loading of polycaprolactone ¹¹. The scaffolds containing low concentration of MCC as a functional additive have improved mechanical properties (in terms of flexural and compression modulus) and simultaneously show an increased cell affinity.

Therefore, this combination have a great potential to be used as scaffolding material in bone regeneration.

Conclusions

This study offers an innovative composite material to manufacture 3D printed scaffolds with potential applications for bone regeneration. The loading with microcrystalline cellulose has a reinforcement effect when the concentration is low (2-5%). The reinforcement effect is related with the increase of crystallinity confirmed by the calorimetric data, the FTIR evaluation and the values of the bulk density of the composites. It is important to highlight that the values of the compressive modulus, the pore size and the apparent density of the scaffolds are similar to those reported for natural spongy bone, so these structures have the potential to be used in the regeneration of this type of tissue.

On the other hand, the loading of microcrystalline cellulose not only improves the mechanical properties of the structure, but also enhances sheep bone marrow cells proliferation for the samples containing 2% w/w of microcrystalline cellulose. However, as the samples with higher content of the additive do not show a similar trend, it would be desirable to carry out a deeper biological assessment in order to identify the mechanism that improves the proliferation at low values of concentration of this additive.

Acknowledgments

The authors thank the European Commission for the funding from the project BAMOS (H2020-MSCA-RISE-2016-734156). M.E. Alemán-Domínguez would like to express her gratitude for the funding through the PhD Grant Program of ULPGC (Code of the grant: PIFULPGC-2014-ING-ARQU-2).

References

1. Petersen PE, Yamamoto T. Improving the oral health of older people: The approach of the WHO Global Oral Health Programme. *Community Dentistry and Oral Epidemiology* 2005;33(2):81-92.
2. Yang GH, Kim M, Kim G. Additive-manufactured polycaprolactone scaffold consisting of innovatively designed micro-sized spiral struts for hard tissue regeneration. *Biofabrication* 2017;9(1).

3. Mondal D, Griffith M, Venkatraman SS. Polycaprolactone-based biomaterials for tissue engineering and drug delivery: Current scenario and challenges. *International Journal of Polymeric Materials and Polymeric Biomaterials* 2016;65(5):255-265.
4. Lebourg M, Martínez-Díaz S, García-Giralt N, Torres-Claramunt R, Ribelles JLG, Vila-Canet G, Monllau JC. Cell-free cartilage engineering approach using hyaluronic acid-polycaprolactone scaffolds: A study in vivo. *Journal of Biomaterials Applications* 2014;28(9):1304-1315.
5. Suwanton O. Biomedical applications of electrospun polycaprolactone fiber mats. *Polymers for Advanced Technologies* 2016;27(10):1264-1273.
6. Correia TR, Ferreira P, Vaz R, Alves P, Figueiredo MM, Correia IJ, Coimbra P. Development of UV cross-linked gelatin coated electrospun poly(caprolactone) fibrous scaffolds for tissue engineering. *International Journal of Biological Macromolecules* 2016;93:1539-1548.
7. Ozdil D, Aydin HM. Polymers for medical and tissue engineering applications. *Journal of Chemical Technology and Biotechnology* 2014;89(12):1793-1810.
8. Mirhosseini MM, Haddadi-Asl V, Zargarian SS. Fabrication and characterization of hydrophilic poly(ϵ -caprolactone)/pluronic P123 electrospun fibers. *Journal of Applied Polymer Science* 2016;133(17).
9. Mehr NG, Li X, Chen G, Favis BD, Hoemann CD. Pore size and LbL chitosan coating influence mesenchymal stem cell in vitro fibrosis and biomineralization in 3D porous poly(ϵ -caprolactone) scaffolds. *Journal of Biomedical Materials Research - Part A* 2015;103(7):2449-2459.
10. Torres E, Fombuena V, Vallés-Lluch A, Ellingham T. Improvement of mechanical and biological properties of Polycaprolactone loaded with Hydroxyapatite and Halloysite nanotubes. *Materials Science and Engineering: C* 2017;75:418-424.
11. Ródenas-Rochina J, Ribelles JLG, Lebourg M. Comparative study of PCL-HAp and PCL-bioglass composite scaffolds for bone tissue engineering. *Journal of Materials Science: Materials in Medicine* 2013;24(5):1293-1308.
12. Song J, Gao H, Zhu G, Cao X, Shi X, Wang Y. The preparation and characterization of polycaprolactone/graphene oxide biocomposite nanofiber scaffolds and their application for directing cell behaviors. *Carbon* 2015;95:1039-1050.
13. Fujihara K, Kotaki M, Ramakrishna S. Guided bone regeneration membrane made of polycaprolactone/calcium carbonate composite nano-fibers. *Biomaterials* 2005;26(19):4139-4147.
14. Liang JZ, Duan DR, Tang CY, Tsui CP, Chen DZ, Zhang SD. Tensile properties of polycaprolactone/nano-CaCO₃ composites. *Journal of Polymer Engineering* 2014;34(1):69-73.
15. Pereira IHL, Ayres E, Averous L, Schlatter G, Hebraud A, De Paula ACC, Viana PHL, Goes AM, Oréfice RL. Differentiation of human adipose-derived stem cells seeded on mineralized electrospun co-axial poly(ϵ -caprolactone) (PCL)/gelatin nanofibers. *Journal of Materials Science: Materials in Medicine* 2014;25(4):1137-1148.
16. Jia B, Li Y, Yang B, Xiao D, Zhang S, Rajulu AV, Kondo T, Zhang L, Zhou J. Effect of microcrystal cellulose and cellulose whisker on biocompatibility of cellulose-based electrospun scaffolds. *Cellulose* 2013;20(4):1911-1923.
17. Bajsić EG, Bulatović VO, Slouf M, Šitum A. Characterization of Biodegradable Polycaprolactone Containing Titanium Dioxide Micro and Nanoparticles. *International Journal of Chemical, Molecular, Nuclear, Materials and Metallurgical Engineering* 2014;8(7).
18. Phillipson K. Ageing and crystallisation of polycaprolactone. United Kingdom: University of Birmingham; 2014.
19. Domingos M, Intranuovo F, Gloria A, Gristina R, Ambrosio L, Bártolo PJ, Favia P. Improved osteoblast cell affinity on plasma-modified 3-D extruded PCL scaffolds. *Acta Biomaterialia* 2013;9(4):5997-6005.

20. Murphy SH, Leeke GA, Jenkins MJ. A Comparison of the use of FTIR spectroscopy with DSC in the characterisation of melting and crystallisation in polycaprolactone. *Journal of Thermal Analysis and Calorimetry* 2012;107(2):669-674.
21. Honma T, Senda T, Inoue Y. Thermal properties and crystallization behaviour of blends of poly(ϵ -caprolactone) with chitin and chitosan. *Polymer International* 2003;52(12):1839-1846.
22. Díez-Pascual AM, Díez-Vicente AL. Electrospun fibers of chitosan-grafted polycaprolactone/poly(3-hydroxybutyrate-co-3-hydroxyhexanoate) blends. *Journal of Materials Chemistry B* 2016;4(4):600-612.
23. Elzein T, Nasser-Eddine M, Delaite C, Bistac S, Dumas P. FTIR study of polycaprolactone chain organization at interfaces. *Journal of Colloid and Interface Science* 2004;273(2):381-387.
24. Senedese ALC, Filho ALL, Lopes da Silva JV, Neto PI, Sena Pereira F, Filho RM. Additive manufacturing to build polycaprolactone scaffolds. 2011; Brazil.
25. Chen C, Yu PHF, Cheung MK. Hydrogen bonding, miscibility, crystallization, and thermal stability in blends of biodegradable polyhydroxyalkanoates and polar small molecules of 4-tert-butylphenol. *Journal of Applied Polymer Science* 2005;98(2):736-745.
26. Olubamiji AD, Izadifar Z, Si JL, Cooper DML, Eames BF, Chen DXB. Modulating mechanical behaviour of 3D-printed cartilage-mimetic PCL scaffolds: Influence of molecular weight and pore geometry. *Biofabrication* 2016;8(2).
27. Fayyazbakhsh F, Solati-Hashjin M, Keshtkar A, Shokrgozar MA, Dehghan MM, Larijani B. Novel layered double hydroxides-hydroxyapatite/gelatin bone tissue engineering scaffolds: Fabrication, characterization, and in vivo study. *Materials Science and Engineering: C* 2017;76:701-714.
28. Hejna A, Formela K, Saeb MR. Processing, mechanical and thermal behavior assessments of polycaprolactone/agricultural wastes biocomposites. *Industrial Crops and Products* 2015;76:725-733.
29. Ruseckaite RA, Jiménez A. Thermal degradation of mixtures of polycaprolactone with cellulose derivatives. *Polymer Degradation and Stability* 2003;81(2):353-358.
30. Alemán-Domínguez ME, Ortega Z, Benítez AN, Vilariño-Feltrer G, Gómez-Tejedor JA, Vallés-Lluch A. Tunability of polycaprolactone hydrophilicity by carboxymethyl cellulose loading. *Journal of Applied Polymer Science* 2018;135(14).
31. Ostrowska B, Di Luca A, Moroni L, Swieszkowski W. Influence of internal pore architecture on biological and mechanical properties of three-dimensional fiber deposited scaffolds for bone regeneration. *Journal of Biomedical Materials Research - Part A* 2016;104(4):991-1001.
32. Chuenjittkuntaworn B, Inrung W, Damrongsri D, Mekaapiruk K, Supaphol P, Pavasant P. Polycaprolactone/hydroxyapatite composite scaffolds: Preparation, characterization, and in vitro and in vivo biological responses of human primary bone cells. *Journal of Biomedical Materials Research - Part A* 2010;94(1):241-251.
33. Gómez-Lizárraga KK, Flores-Morales C, Del Prado-Audelo ML, Álvarez-Pérez MA, Piña-Barba MC, Escobedo C. Polycaprolactone- and polycaprolactone/ceramic-based 3D-bioprinted porous scaffolds for bone regeneration: A comparative study. *Materials Science and Engineering: C* 2017;79(Supplement C):326-335.
34. Chen B, Sun K. Mechanical and dynamic viscoelastic properties of hydroxyapatite reinforced poly(ϵ -caprolactone). *Polymer Testing* 2005;24(8):978-982.
35. Naganuma T. The relationship between cell adhesion force activation on nano/micro-topographical surfaces and temporal dependence of cell morphology. *Nanoscale* 2017;9(35):13171-13186.
36. Yao X, Peng R, Ding J. Cell-material interactions revealed via material techniques of surface patterning. *Advanced Materials* 2013;25(37):5257-5286.
37. Nikkhah M, Edalat F, Manoucheri S, Khademhosseini A. Engineering microscale topographies to control the cell-substrate interface. *Biomaterials* 2012;33(21):5230-5246.

38. Verrier S, Blaker JJ, Maquet V, Hench LL, Boccaccini AR. PDLLA/Bioglass® composites for soft-tissue and hard-tissue engineering: an in vitro cell biology assessment. *Biomaterials* 2004;25(15):3013-3021.

Figure captions

Figure 1. FTIR spectrum of PCL and the composite materials.

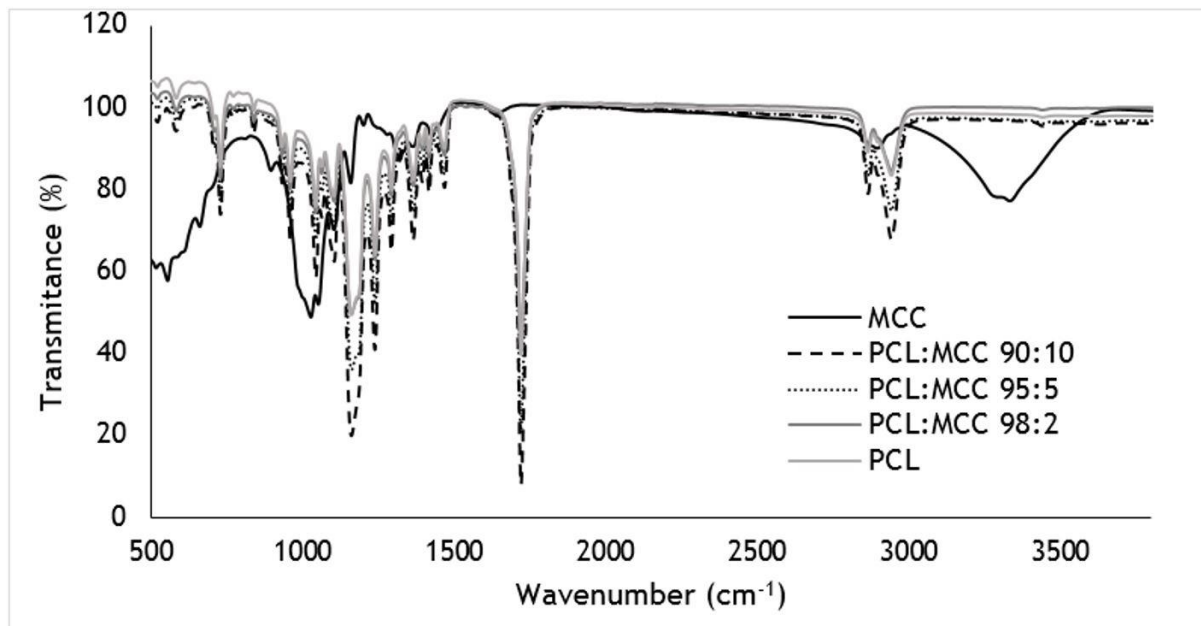


Figure 2. SEM images of PCL and composite scaffolds (a-PCL, b-PCL:MCC 98:2, c-PCL:MCC 95:5 and d-PCL:MCC 90:10).

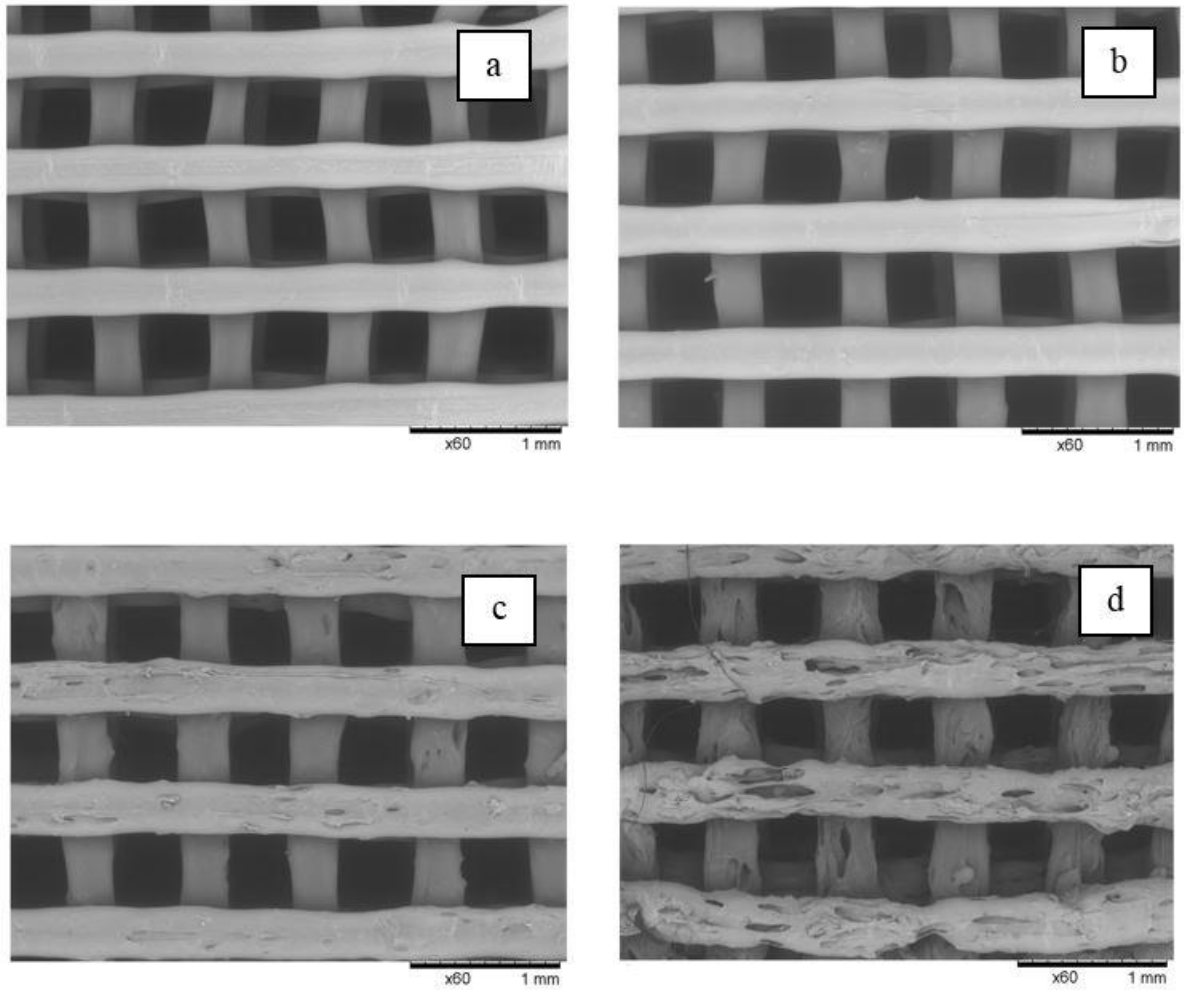


Figure 3. Mechanical properties under 3 point bending testing (* $p < 0.05$ compared to the group of pure PCL samples).

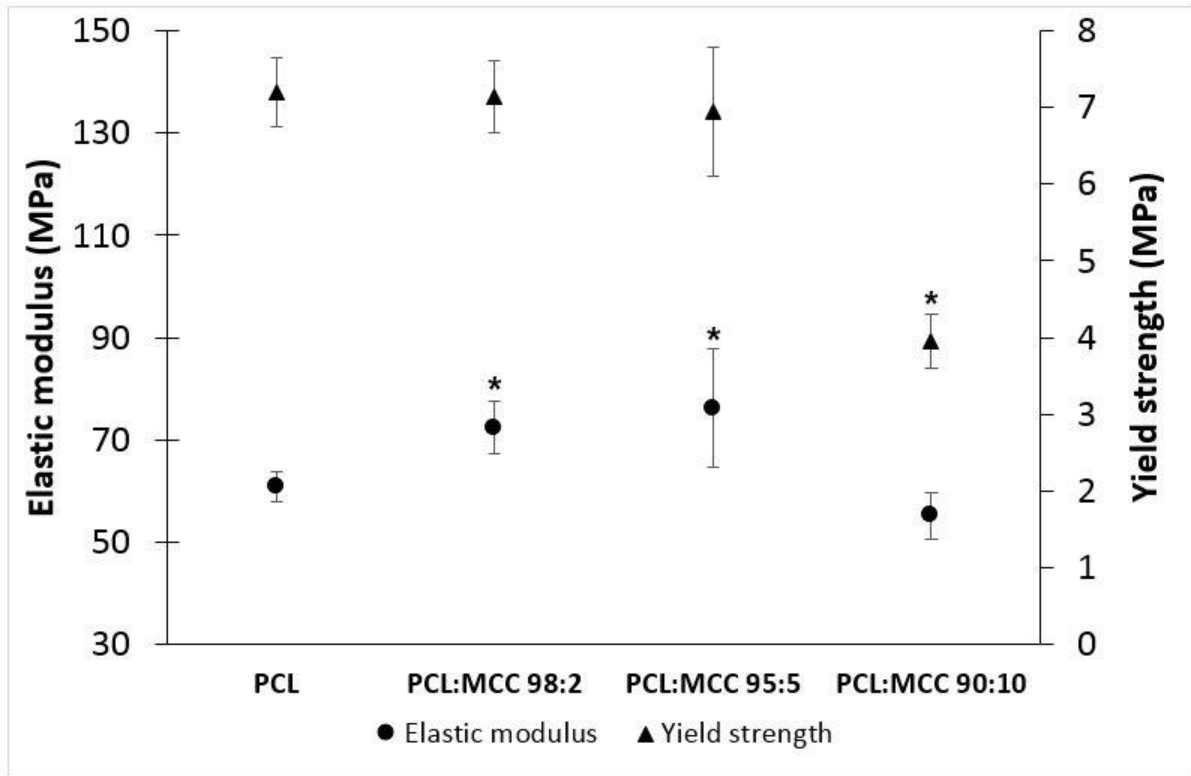


Figure 4. Mechanical properties under compression testing (* $p < 0.05$ compared to the group of pure PCL samples).

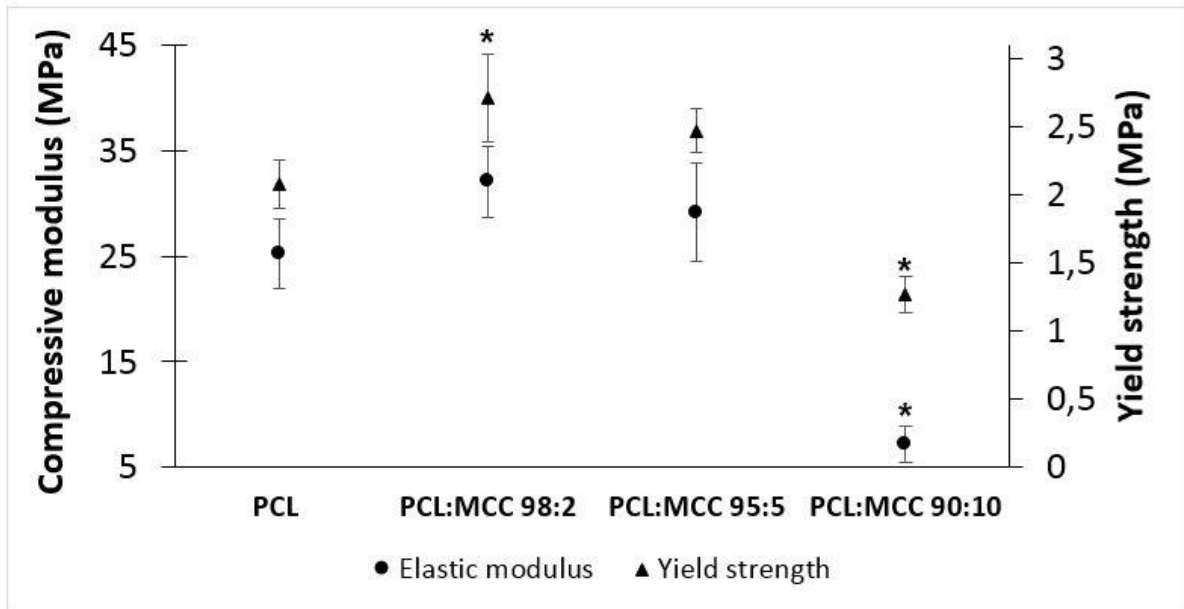


Figure 5. Results of viability tests for PCL:MCC composites using Presto Blue ® assay (* p<0.05 compared to the group of pure PCL samples).

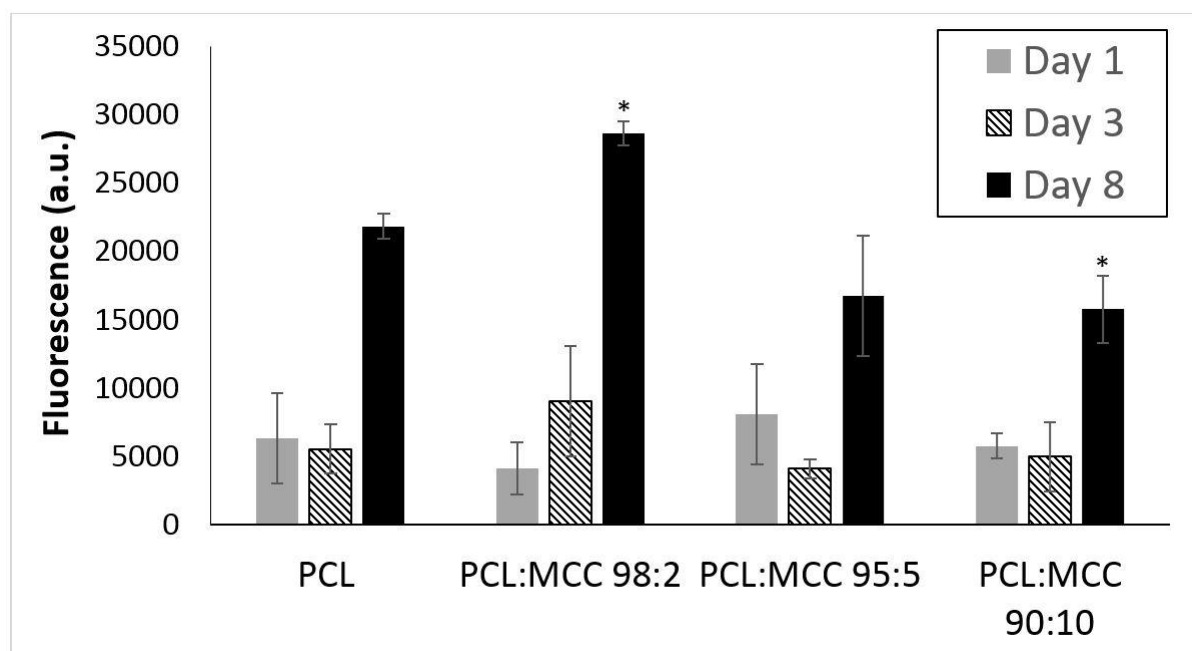


Table 1. Values of the maximum degradation rate temperature, melting temperature and enthalpy of fusion for polycaprolactone, microcrystalline cellulose and their composites.

Material	Maximum degradation rate temperature (°C)	Melting temperature (°C)	Enthalpy of fusion (J/g)	Degree of crystallinity (%)
PCL	430	63	33	23
PCL:MCC 98:2	424	68	39	28
PCL:MCC 95:5	424	70	43	31
PCL: MCC 90:10	424	68	38	30

Table 2. Ratio of the FTIR peak areas (CH₂ in the amorphous phase/C-O-C in the crystalline phase) (* p<0.05; **p<0.01; ***p<0.001 compared to the group of pure PCL samples).

Material	Ratio of areas (CH ₂ peak at 2945 cm ⁻¹ / C-O-C peak at 1245 cm ⁻¹)
PCL	1.34
PCL:MCC 98:2	1.08**
PCL:MCC 95:5	1.19*
PCL:MCC 90:10	1.14

Table 3. Values of the bulk density of the materials evaluated and porosity values of the 3D printed scaffolds (* p<0.05; **p<0.01; ***p<0.001 compared to the group of pure PCL samples).

Material	Bulk density (g/cm ³)	Apparent density (g/cm ³)	Porosity (%)	Distance between filaments (μm)
PCL	1.09±0.02	0.52±0.03	52±2	463±26
PCL:MCC 98:2	1.16±0.03**	0.53±0.02	54±1	470±36
PCL:MCC 95:5	1.23±0.02***	0.48±0.03	58±3**	482±31*
PCL: MCC 90:10	1.13±0.02**	0.49±0.03	57±2*	448±54

